RSC Advances

ROYAL SOCIETY OF CHEMISTRY

www.rsc.org/advances

Synthesis and characterization of starch/AlOOH/FeS_2 nanocomposite for the adsorption of congo red dye from aqueous solution

Rajeev Kumar,[a*] J. Rashid,[a] M.A. Barakat[a,b,c]

[a]*Department of Environmental Sciences, Faculty of Meteorology, Environment and Arid Land Agriculture, King Abdulaziz University, Jeddah, 21589, Saudi Arabia*

[b]*Central Metallurgical R & D Institute, Helwan, 11421, Cairo, Egyp*

[c]*Center of Excellent in Environmental Studies (CEES), King Abdulaziz University*

*Corresponding Author: Rajeev Kumar

Email: olifiaraju@gmail.com

Tel.: +966 (02)6400000/64821

Fax: +966(02) 6952364

Abstract

This work described the synthesis and characterization of starch/AlOOH/FeS_2 nanocomposite for the adsorption of congo red (CR) dye from aqueous solution. The morphology of the starch/AlOOH/FeS_2 was characterized by using scanning and transmission electron microscopy, N_2 adsorption-desorption isotherm, X-ray photoelectron spectroscopy, fourier transform-infrared spectroscopy. The adsorption of CR onto starch/AlOOH/FeS_2 was evaluated as a function of contact time, solution pH, concentration and temperature. Adsorption results demonstrate that the maximum removal of CR was found to be at pH 5. The adsorption kinetics data fitted well to the pseudo first-order equation whereas Freundlich equation exhibits the better correlation to the experimental data. Thermodynamic parameters, such as standard free energy change (ΔG°), standard entropy change (ΔS°) and standard enthalpy change (ΔH°), were also evaluated. The results suggested that starch/AlOOH/FeS_2 is a potential adsorbent for the CR dye removal from aqueous solution.

Introduction

Organic dyes and pigments discharged from textile, cosmetics, food, pharmaceutical, paper etc. industries are serious environmental problems because their unwanted colour and resistance to decompose. Synthetic dyes are toxic and carcinogenic in nature to the organism and mammals [1, 2]. Congo red (CR) (sodium salt of benzidinediazobis-1-naphthylamine- 4-sulfonic acid) is wieldy used in textile, leather, paper, printing industries etc. and around 15 % CR discharged in wastewater during operation. CR is well known carcinogenic and its exposure may cause some allergic responses [2,3]. Moreover, due to its complex aromatic, eliminate or degrade (bio/photo) of CR from aqueous medium by conventional methods is difficult. Several methods such as adsorption, oxidation, photocatalysis, membrane filtration, biological degradation etc. have been used for the treatment of dyeing effluents [1,4-7]. Among all them, adsorption is a very promising method for the removal of dyes from wastewater. Several adsorbents such as carbons, metal oxides, polymers, clays, composites etc. have been used for the removal of CR from aqueous solutions [1,2,4, 8-10]. However, low or moderate adsorption capacities of these materials towards the CR removal promote the researchers to develop novel materials with high efficiency and economical removal of CR from dyeing effluents.

The recently discovered hybrid materials showed many advantages in wastewater treatment [3]. The adsorption ability of hybrid materials relies on the smart manipulation of the structure of the embedded compounds such as charge, functionality, hydrophobic-hydrophilic nature etc. [5]. Boehmite (AlOOH) is non-hazardous material, exhibit good adsorption capacity (85-99 mg g^{-1}) toward CR from aqueous solution [11].The adsorption of the CR onto AlOOH takes place due to interaction between metal sites and amine group of dye. The adsorption performance

of AlOOH can be enhanced by tailoring its surface. The high functionality of starch and pyrite combined with AlOOH can much effectively remove the CR from wastewater. Pyrite and starch are most abundant sulfide mineral and biopolymer, respectively. Starch and starch based adsorbent have been investigated for the removal of various classes of dyes [12-14]. To the best of our knowledge, Pyrite or pyrite based adsorbent has not been investigated for the removal of dyes. However, few studies were reported for the removal of metal ions such as molybdate, tetrathiomolybdate, [15], Cu(II), Cd(II) and Pb(II) [16], As(III)) and As(V) [17],etc. Pyrite showed good adsorption capacity for negatively charged metal ions. Therefore, it is supposed to be good adsorbent for the removal of negatively charged CR dye. In this work, a simple route for the synthesis of starch/AlOOH/FeS_2 composite and its adsorption efficiency for the removal of CR is reported. The adsorption of CR onto starch/AlOOH/FeS_2 is discussed in terms of kinetics, thermodynamics and isotherm studies.

Materials and methods

Materials

Starch (potato) and aluminum nitrate were purchased from Panreac Quimica S.A. Congo red and Sodium dodecyl sulfate (SDS) were obtained from Techno Pharmachem Haryana, India and Scharlab S.L. Spain. $FeSO_4.7H_2O$ and NH_4HCO_3 were supplied by BDH chemical Ltd and Fisher Scientific Company, New Jersey.

Synthesis of starch/AlOOH/FeS_2nanocomposite

In a typical synthesis, 13.9 g $Al_2(NO_3)_3$ was dissolved in 25 ml water under sonicated (Elma S30H Elmasonic) for 20 min, and then 1 g starch was added into the

solution. After sonication at 40 °C for 30 min, 1.2 g SDS was added into the solution to prevent the agglomeration of particles. Thereafter, 100 ml 2.0 M NH_4HCO_3 was added to the mixture and sonicated for 2 h at 60 °C. Resulting white precipitate was filtered by Buchner funnel with a sintered glass disk and thoroughly washed with hot de-ionized water and ethanol for the removal of excess starch and SDS. The obtained white precipitate was transferred into ethanol solution (200 mL) containing 8.0 g $Na_2S_2O_3$ and 4.4 g $FeSO_4.7H_2O$ under sonication at 40 °C for 30 min. Thereafter, the mixture was refluxed at 180 °C for 1 h and finally cooled to room temperature. The precipitate was filtered and thoroughly washed with hot de-ionized water and ethanol, and dried at 200 °C for 4 h. Dry sample was collected and stored for further adsorption studies.

Characterization

The morphology of starch/AlOOH/FeS_2 was investigated by field emission scanning electron microscopy (FESEM) (JSM-7500 F; JEOL–Japan) without spurting coated gold or carbon and transmission electron microscopy (TEM) (model Tecnai G2 F20 Super Twin) at 200 kV with LaB_6 emitter. X-ray photoelectron spectroscopy (XPS) measurements were recorded on SPECS GmbH, (Germany) spectrometer operated at a base pressure of 10^{-10} mbar and step size 1 eV. A non-monochromatic Mg- Kα (1253.6 eV) X-ray source was used to irradiate the sample surface with 13.5 kV, 100 W X-ray power. The nitrogen adsorption–desorption isotherm analysis [Brunauer, Emmett and Teller (BET) and Density Functional Theory (DFT)] of starch/AlOOH/FeS_2 was performed at 77 K Quantachrome Nova Win 2 (Quantachrome instruments) equipment by degassing the sample at 200 °C. FTIR

spectra of starch/AlOOH/FeS_2 before and after CR adsorption were recorded using a Perkin Elmer Spectrum 100 FTIR Spectrometer over a range of 500 – 4000 cm^{-1}.

Adsorption Studies

Adsorption of CR was investigated under a wide variety of experimental conditions. A series of experiments were performed by reacting 0.02 g starch/AlOOH/FeS_2 with 20 mL of CR solution (50-500 mg L^{-1}) as a function of solution pH ranging from 5-9. The solution pH was adjusted using 0.1 M HCl and NaOH. Adsorption isotherms were performed at pH 5, 7, 9 and at temperature 30, 40, 50 °C. The effect of contact time was studied in a series of flasks contain 20 mL dye solution of 500 mg L^{-1} in water bath shaker at 200 rpm at temperature 25, 40, 50 °C. After a fixed time interval, the samples were filtered and the amount of dye remaining in the supernatant solution was analyzed using a HACH LANGES DR-6000 UV-visible spectrophotometer at 495 nm. The amount of CR adsorbed on starch/AlOOH/FeS_2 can be estimated by:

$$q_e = (C_0\text{-}Ce)V/m \quad (1)$$

where, q_e is the amount of CR adsorbed per unit mass of starch/AlOOH/FeS_2 (mg g^{-1}), C_0 and Ce is the initial and equilibrium dye concentration (mg L^{-1}), respectively. V is the volume of dye solution (L) and m is the mass of starch/AlOOH/FeS_2 (g).

Results and Discussion

Characterization

The morphology of the prepared composite material was investigated by SEM and TEM as shown in Fig. 1. The SEM images (Fig. 1a) shows the needle like clusters of starch/AlOOH/FeS_2. The TEM image (Fig. 1b) also reflects the needle like

structure. The high resolution TEM image (Fig. 1c) shows the polycrystalline nature of starch/AlOOH/FeS_2 composite.

The specific BET surface area and pore structure of the starch/AlOOH/FeS_2 was investigated using N_2 adsorption–desorption measurements. Fig. 2 shows the type IV isotherm. The BET, DFT surface area and total pore volume are 40.013, 25.33 and 0.055 m^2/g, respectively. The pore diameter is found to be in the range of 1.348 to 3.39 nm and the total micropore and mesopore are 0.0549 and 0.0484 cm^3/g, respectively. The surface analysis of starch/AlOOH/FeS_2 by XPS is shown in Fig. 3. The sulfur peak located at 163. 82 eV is corresponding to the $2p^{1/2}$ which is identical with the S^{2-} in the pyrite [18]. Broad peaks located at 168.69 and 530 eV are due to the presence of SO_4^{2-} impurities of iron precursor and FeOOH (O 1s). Moreover, the Fe $2p^{3/2}$ and $2p^{1/2}$ peaks are located at 708.2 eV and 719.6 eV are consistent with bulk pyrite [19]. Two peaks appeared at 118.5 eV and 74.68 eV are corresponding to the Al 2s and 2p, and confirm the presence of AlOOH in the composite [20]. The binding energies for C 1s of the starch functional groups at 284.8, 286.6 and 288.38 eV are corresponding to the C–C/C–H, C–O (alcohol) and O–C–O (ester), respectively [21]. In addition, the presence of these functional groups can be confirmed by FTIR analysis of starch/AlOOH/FeS_2 nanocomposite. Fig. 4 shows the FTIR spectra of starch/AlOOH/FeS_2. The broad and strong peaks centered at 3213 and 1633 cm^{-1} are attributed to the O–H vibrations of starch/AlOOH or water. The broad peak at 1079 cm^{-1} can be assigned to the C–O–C linkage of the starch [22,23]. Moreover, the broad peak with small shoulders in the range of 1000-1200 may be attributed to the pyrite [24]. The strong band at 766 cm^{-1} may be ascribed to the AlO_6 vibration mode which shifted to 757 cm^{-1} after adsorption. After dye adsorption new peaks appear in the region 1500-1600 and 1417, 1371, 1040 cm^{-1} may be assign to the NH, NH_2 and C–H

(bending), S–O (stretching) vibrations of the dye [2, 25, 26]. From the FTIR spectra, it is noted that most of the peaks shifted or diminished after the adsorption of dye. The shift in wave numbers and intensity of the peaks could be due to the interaction of dye functional groups (NH, NH_2, SO_3^-) with the adsorbent functional groups [2].

Effect of solution pH

CR is highly sensitive to the solution pH and shows colour change from red (λ_{max} – 496 nm) to blue (λ_{max} – 580 nm) in the presence of inorganic acids in the pH ranges from 2-4 due protonation of azo group (π –π transition) [2,8]. Fig. 5 shows the pH dependent adsorption of CR onto starch/AlOOH/FeS_2 nanocomposite. The adsorption of CR decreases with the increase in the solution pH from 5 to 9 and maximum adsorption isfound to be at pH 5 as shown in Fig. 5. The adsorptive removal of CR shows a slight decrease at pH 9 compared to pH 7. Several investigations revealed that adsorption of negatively charged CR usually increases as the solution pH decreased [2,8, 27]. This behavior can be explained on the basis of change in the functionality of adsorbent with respect to the solution pH. According to Gissinger et al., [28], S–S–H groups are predominated in acidic medium and pyrite surface shows a deficiency of iron and formation of iron vacancies $Fe_{1-X}S_2$, while O–H groups are predominated in basic medium. When the solution pH increases, the pyrite surface shows the excess of FeOOH. Both S–S–H and O-H groups are coexisting over the entire pH range at pyrite surface. Therefore, high adsorption is observed in acidic medium and both groups are thus probably involved in the binding of CR by the surface complexation. The adsorbent shows effective removal of CR at natural and basic condition (pH 9). This may be explain on the basis of positive surface charge of AlOOH (in basic medium at pH<10) while CR is anionic charged.

Thus, CR is electrostatically adsorbed on adsorbent surface (Dye–SO_3^- + $AlOOH_2^+$↔ Dye–SO_3^-·····$^+H_2OOAl$) [27, 29]. Furthermore, CR may be adsorbed on the surface of metal oxides due to a coordination effect of metal atoms with –NH_2 and –SO_3^- groups of CR. Moreover, the adsorption of CR may be largely ascribed to the strong hydrogen bond formed between the electronegative atoms of dye and adsorbent such as oxygen, nitrogen or sulfur and hydrogen atoms [9]. From the results mentioned above and previous reports [9,10, 27] hydrogen bonding, electrostatic interaction, complexation and coordination effect of metal atoms with –NH_2 and –SO_3^- groups are mainly responsible for the adsorption of CR in neural CR solution. Therefore, pH 7 is selected for the further adsorption studies.

Adsorption kinetics

The Effect of contact time on CR adsorption is shown in Fig. 6. The removal of CR is very fast during the first 100 min due to the adsorption of dye molecules onto the vacant adsorbent sites and thereafter rate of dye adsorption decreases due to the saturation of active sites (internal surface adsorption) [2]. The equilibrium is attained within 300 min. Adsorption dynamics of CR removal on starch/AlOOH/FeS_2 are performed to find the rate controlling step. The adsorption data has been analyzed using pseudo first-order and pseudo second-order kinetic models. The linear equations for pseudo first-order [30] and pseudo-second order [31] kinetic models, respectively, are given as:

$$\log(q_e - q_t) = \log q_e - (k_1\, t/2.303) \quad (2)$$

$$t/q_e = (1/k_2 q_e^2) + t/q_e \quad (3)$$

where and q_e (mg g^{-1}) and q_t (mg g^{-1}) refer to the adsorption capacity at equilibrium and after time t (min) respectively. k_1 (min^{-1}) and k_2 (g mg^{-1} min^{-1}) are the pseudo-

first and pseudo-second order rate constant, respectively. The values for pseudo first-order and pseudo second-order kinetic parameters obtained from their respective linear plots $\log(q_e - q_t)$ against t and t/q_e against t, respectively are tabulated in Table 1. The calculated adsorption capacities (q_e^{cal}) from pseudo first order kinetic equation are close to the experimental (q_e^{exp}) values. Furthermore, R^2 values obtained for pseudo first-order kinetic equation are higher than pseudo second-order kinetic equation. These results revealed that the ongoing adsorption reaction proceeds via a pseudo-first order kinetic rather than a pseudo second-order kinetic mechanism. Similar type of adsorption behavior for CR adsorption onto bio-polymeric composite was reported by Chatterjee et al., [3] and Duet. al., [32].

Adsorption isotherms

The adsorption isotherms analysis has been performed at different concentrations and temperatures as shown in Fig. 7. The removal of CR increases with the increases in solution concentration and temperature. This can be due to the greater driving force through a higher concentration gradient at high concentration [2]. An increase in the temperature, enhance the mobility of the dye molecule and decrease in the retarding forces acting on the diffusing dye molecules. This results in the increase in the adsorption capacity of starch/AlOOH/FeS_2 for CR [33].

In attempting to describe the adsorption isotherm of CR removal by starch/AlOOH/FeS_2, Langmuir, Freundlich and Temkin isotherm models are tested. The linear equation for Langmuir [34], Freundlich [35] and Temkin [36] isotherm models, respectively are given as:

$$1/q_e = (1/q_m b C_e) + 1/q_m \quad (4)$$

$$\ln q_e = \ln K_F + (1/n) \ln C_e \quad (5)$$

$$q_e = B \ln A + B \ln C_e \quad (6)$$

where q_e (mg g^{-1}) and C_e (mg L^{-1}) are the CR adsorption capacity and concentration at equilibrium, q_m (mg g^{-1}) and b (L mg^{-1}) are Langmuir constant. Freundlich isotherm constants K_F ($mg^{1-1/n}$ $L^{1/n}g^{-1}$) and n are representing the capacity and intensity of adsorption. Temkin isotherm parameters, A (L mg^{-1}) and B are related to the equilibrium binding constant and the heat of adsorption, respectively. The parameters for Langmuir, Freundlich and Temkin isotherms are calculated for their respective linear plots $1/q_e$ vs. $1/C_e$, $\ln q_e$ vs. $\ln C_e$ and q_e vs. $\ln C_e$. From the Table 2, it can be seen that the values of correlation coefficient (R^2) for the Freundlich isotherm model are higher than the Langmuir and Temkin adsorption models, revealing that experimental equilibrium data fits better with Freundlich isotherm. This reveled that adsorption of CR occur through multilayer formation on the heterogeneous surface of starch/AlOOH/FeS_2composite [37]. Moreover, the magnitude of Freundlich constant (n) should be more than one for favorable adsorption process [38-39]. The values of n (Table 2) are greater than one at all the studied temperatures revealing the feasible adsorption of CR onto starch/AlOOH/FeS_2 composite.

Adsorption thermodynamics

The adsorption of CR onto starch/AlOOH/FeS_2 increases from 298 mg g^{-1} to 346 mg g^{-1} with the increase in solution temperature from 30 °C to 50 °C as shown in Fig. 7. These results indicate that the adsorption of process is endothermic in nature. Adsorption thermodynamic parameters for CR removal, standard Gibbs free energy change (ΔG°), standard entropy change (ΔS°) and standard enthalpy change (ΔH°) are calculated from following equations:

$$\Delta G° = - RT \ln K_c \quad (7)$$

$$Kc = (C_{ae}/C_e) \quad (8)$$

$$\ln K_c = (\Delta S°/R) - (\Delta H°/RT) \quad (9)$$

where, K_c and R (8.314 J mol^{-1} K^{-1}) are the distribution coefficient and gas constant, respectively. T is the temperature (K). C_{ae} and C_e are the equilibrium concentration of CR (mg g^{-1}) on adsorbent and in solution, respectively. The value of ΔH° and ΔS° calculated from the slope and intercept of ln K_c verses 1/T are in Table 3. As can be seen from Table 3, the values of ΔG° are negative indicating the feasibility and spontaneous nature of adsorption process for all the studied temperatures. The positive value of ΔH° and ΔS° confirming the endothermic process and increase in randomness at solid/solution interface [40]. To a certain extent, the forces involve in the adsorption process can be determined by the magnitude of ΔH° and ΔG°. For the physisorption, the ΔG° value should be lower than −20 kJ mol^{-1} and those for chemisorptions ranges from −80 to −400 kJ mol^{-1}. The ΔG° values for CR adsorption are in the range of −0.891 to −2.172 kJ mol^{-1}, indicating that physical forces are involved in CR adsorption onto starch/AlOOH/FeS_2. The energy (ΔH°) associated with physisorption: van der Waals forces (4–10 kJ mol^{-1}), hydrophobic interaction (5 kJ mol^{-1}), hydrogen bonding (2–40 kJ mol^{-1}), coordination exchange (40 kJ/mol), dipole bond forces (2–29 kJ mol^{-1}), and electrostatic interaction (20-80 kJ mol^{-1}), while for chemisorptions bond strength can be ranges from 80 to 450 kJ mol^{-1}[40, 41]. The value of ΔH° is 17 kJ mol^{-1} confirming the involvement of physical forces in CR adsorption.

Conclusion

This article described the facile method for the synthesis of starch/AlOOH/FeS_2 nanocomposite for the high efficient removal of CR from aqueous solution. The prepared material shows good surface area with the mesoporous structure. FTIR analysis shows that the NH, NH_2 and SO_3^- groups are involved in the interaction of dye on the surface of starch/AlOOH/FeS_2. The adsorption results demonstrate that CR removal is highly dependent on the solution pH, contact time, concentration and temperature. Adsorption isotherm study revealed that surface of starch/AlOOH/FeS_2 is heterogeneous and multilayer adsorption of CR supposes to occur on the adsorbent surface. Thermodynamic study suggested that adsorption of CR onto starch/AlOOH/FeS_2 is spontaneous and endothermic in nature. The magnitude of standard Gibbs free energy change ($\Delta G°$), and standard enthalpy change ($\Delta H°$) revealed that the physical forces are involved in the adsorption of CR onto starch/AlOOH/FeS_2 surface. These results therefore suggested that starch/AlOOH/FeS_2 can be considered as a potential material for the scavenging of CR from aqueous solution.

References

1. M. Dong, Q. Lin, D. Chen, X. Fu, M. Wang, Q. Wu, X. Chen and Shipu Li. RSC Adv., 2013, 3, 11628–11633.
2. R. Ahmad and R. Kumar, Appl. Surf. Sci., 2010, 257, 1628–1633.
3. S. Chatterjee, M. W. Lee and S. H. Woo, Bioresour. Technol., 2010, 101, 1800–1806.
4. W. Cai, Y. Hu, J. Chen, G. Zhang and T. Xia, Cryst. Eng. Comm., 2012, 14, 972–977.
5. Z. Y. Chen, H. W. Gao and Y. Y. He, RSC Adv., 2013, 3, 5815–5818.
6. M. Solís, A. Solís, H. I. Pérez, N. Manjarrez and M. Flores, Process Biochem.,2012, 47, 1723–1748.
7. E. Forgacsa, T.Cserhatiand G. Oros, Environ. Int., 2004, 30, 953 – 971.
8. M.Toor and B. Jin, Chem. Eng. J., 2012, 187, 79– 88.
9. J. Wu, J. Wang, H. Li, Y. Du, K. Huang and B. Liu, J. Mater. Chem. A, 2013, 1, 9837–9847.
10. A. Mahapatra, B.G. Mishra and G. Hota, Ceram. Int., 2013, 39, 5443–5451.
11. C. Wang, S. Huang, L. Wang, Z. Deng, J. Jin, J. Liu, L. Chen, X. Zheng, Y. Li and B. L. Su, RSC Adv., 2013, 3, 1699–1702.
12. V. Janaki, K. Vijayaraghavan, B. T. Oh, K. J. Lee, K. Muthuchelian, A.K. Ramasamy and S. K. Kannan, Carbohydr.Polym.2012, 90, 1437–1444.
13. P. R. Chang, P. Zheng, B. Liu, D. P. Anderson, J. Yu and X. Ma, J. Hazard. Mater., 2011, 186, 2144–2150.
14. S. Xu, J. Wang, R. Wu, J. Wang and H. Li, Chem. Eng. J., 2006, 117, 161–167.

15. N. Xu, C. Christodoulatos and W. Braida, Chemosphere, 2006, 62, 1726–1735.
16. A. Ozverdi and M. Erdem, J. Hazard. Mater., 2006, 137, 626–632.
17. D. S. Han, J. K. Song, B. Batchelor and A. A. Waha, J. Colloid Interface Sci.,2013, 392, 311–318.
18. S. C. Hsiao, C. M. Hsu, S. Y. Chen, Y. H. Perng, Y. L.Chueh, L. J. Chen and L. H. Chou, Mater. Lett., 2012, 75, 152–154.
19. A. R. Pratt, H. W. Nesbitt and J. R. Mycroft, J. Geochem. Explor., 1996, 56, 1-11.
20. C. Gao, X. Y. Yu, R. X. Xu, J. H. Liuand X. J. Huang, ACS Appl. Mater. Interfaces, 2012, 4, 4672−4682.
21. A. Uliniuca, M. Popa, E. Drockenmuller, F. Boisson, D. Leonard and T. Hamaidea, Carbohydr.Polym.,2013, 96, 259–269.
22. Q. Lin, J. Pan, Q. Lin and Q. Liu, J. Hazard. Mater., 2013, 263, 517– 524.
23. L.O. Filippov V.V. Severov, I.V. Filippova, Int. J. Miner. Process., 2013, 123, 120–128.
24. R. K. Rath, S. Subramanian and T. Pradeep. J. Colloid Interface Sci. 2000, **229,** 82–91.
25. Y. Yang, G. Wang, B. Wang, Z. Li, X. Jia, Q. Zhou and Y. Zhao, Bioresour. Technol., 2011, 102, 828–834.
26. F. Zhang, Y. Liu, Y. Cai, H. Li, X. Cai, I. Djerdj and Y. Wang, Powder Technol.2013, 235, 121–125.
27. Y. Wang, W. Li and X. J. Chen, J. Mater. Chem. A, 2013, 1, 10720–10726.
28. P.B. Gissinger, M. Alnot, J.E. Ehrhardt, P. Behra, Environ. Sci. Technol., 1998, 32, 2839-2845.

29. K. Rezwan, L. P. Meier and L. J. Gauckler, Biomaterials, 2005, 26, 4351–4357.
30. S. Lagergren, K. Sven. Vetenskapsakad. Handl.,1898,24, 1–39.
31. G. McKay and Y. S. Ho, Process Biochem.,1999, 34, 451–465.
32. Q. Du, J. Sun, Y. Li, X. Yang, X. Wang, Z. Wang, L. Xia, Chem. Eng. J., 2014, 245, 99–106.
33. V. S. Mane and P.V. V. Babu, J. Taiwan Inst. Chem. E.,2013, 44, 81–88.
34. I. Langmuir, J. Am. Chem. Soc., 1918, 40, 1361–1403.
35. M. I. Temkinand V. Pyzhev. Acta Physiochemica, 1940, 12, 217–222.
36. H. Freundlich,Uber die adsorption in loseungen, J. Phys. Chem., 1907, 57, 385–470.
37. L. Yu, W. Xue, L. Cui, W. Xing, X. Cao and H. Li, Int. J. Biol. Macromol.,2014, 64, 233– 239.
38. S. Dawood and T. K. Sen, Water Res., 2012, 46, 1933-1946.
39. V. Vimonses, S. Lei, B. Jin, C.W.K. Chow and C. Saint, Chem. Eng. J., 2009, 148, 354-364.
40. S. Liu, Y. Ding, P. Li, K. Diao, X. Tan, F. Lei, Y. Zhan, Q. Li, B. Huang and Z. Huang, Chem. Eng. J.,2014, 248, 135–144.
41. F.M. Machado, C.P. Bergmann, E.C. Lima, B. Royer, F. E. de Souza, I. M. Jauris, T. Calvete and S. B. Fagan, Phys. Chem. Chem. Phys.,2012, 14, 11139–1

Tables

Table 1. Kinetic parameters for CR adsorption onto starch/AlOOH/FeS_2

Temp	$q_e^{(exp)}$	Pseudo-first order model			Pseudo-second order model		
(°C)	(mg g^{-1})	$q_e^{(cal)}$ (mg g^{-1})	k_1 (min^{-1})	R^2	$q_e^{(cal)}$ (mg g^{-1})	k_2 (g mg^{-1} min^{-1})	R^2
25	261	266.07	11.51×10^{-3}	0.994	333.33	3.474×10^{-5}	0.985
40	313.2	305.49	9.212×10^{-3}	0.996	500	1.550×10^{-5}	0.990
50	346.2	320.62	9.212×10^{-3}	0.987	500	19.704×10^{-5}	0.984

Table 2. Adsorption isotherm parameters for CR adsorption onto starch/AlOOH/FeS_2

	Langmuir isotherm model				Freundlich isotherm model			Temkin isotherm model		
Temp. °C	q_m (mg g^{-1})	b (L mg^{-1})	R^2	R_L	K_F ($mg^{1-1/n}$ $L^{1/n}g^{-1}$)	n	R^2	A (L mg^{-1})	B	R
30	333.33	0.032	0.951		44.880	2..288	0.970	0.226	78.06	0.955
40	333.33	0.040	0.957		45.422	2.293	0.980	0.274	81.66	0.970
50	333.33	0.166	0.912		70.035	3.246	0.956	1.455	61.65	0.923

Table 3. Thermodynamic parameters for CR adsorption onto starch/AlOOH/FeS_2

Temperature (°C)	ΔG° kJ mol^{-1}	ΔH° kJ mol^{-1}	ΔS° J $mol^{-1}K^{-1}$	R^2
30	− 0.891			
40	− 1.358	17.002	59.137	0.948
50	− 2.173			

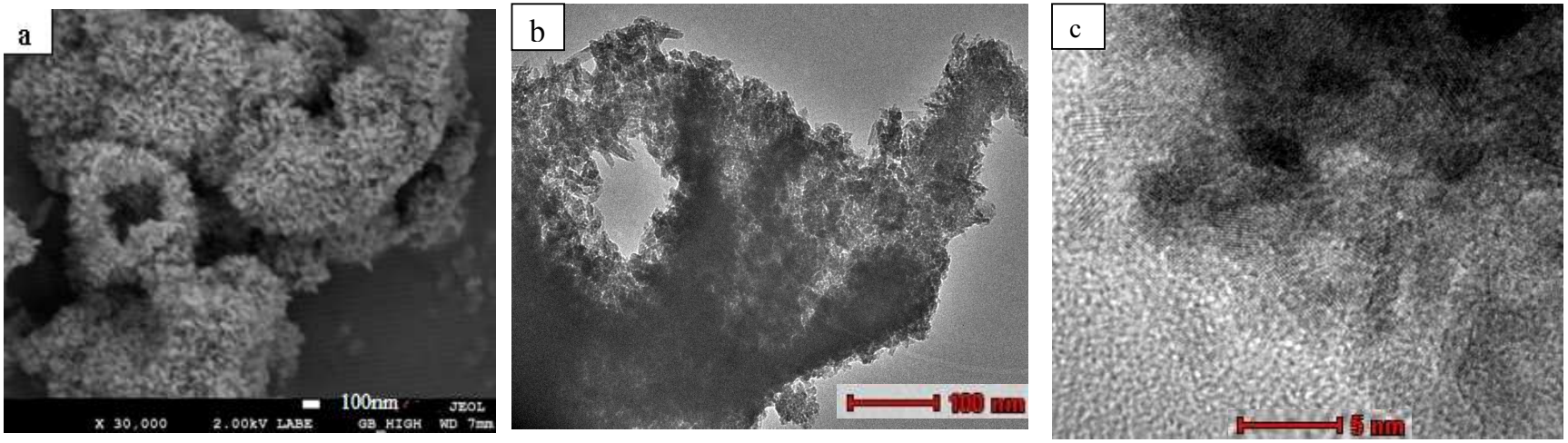

Fig. 1. SEM (a), TEM (b) and HRTEM (c) of starch/AlOOH/FeS_2.

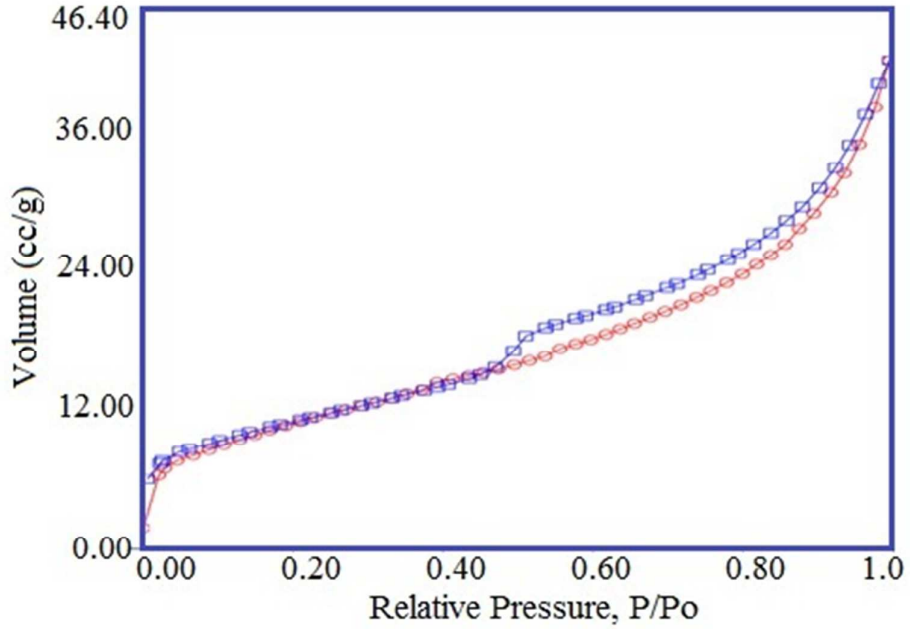

Fig. 2. Nitrogen adsorption-desorption isotherm plot of starch/AlOOH/FeS_2

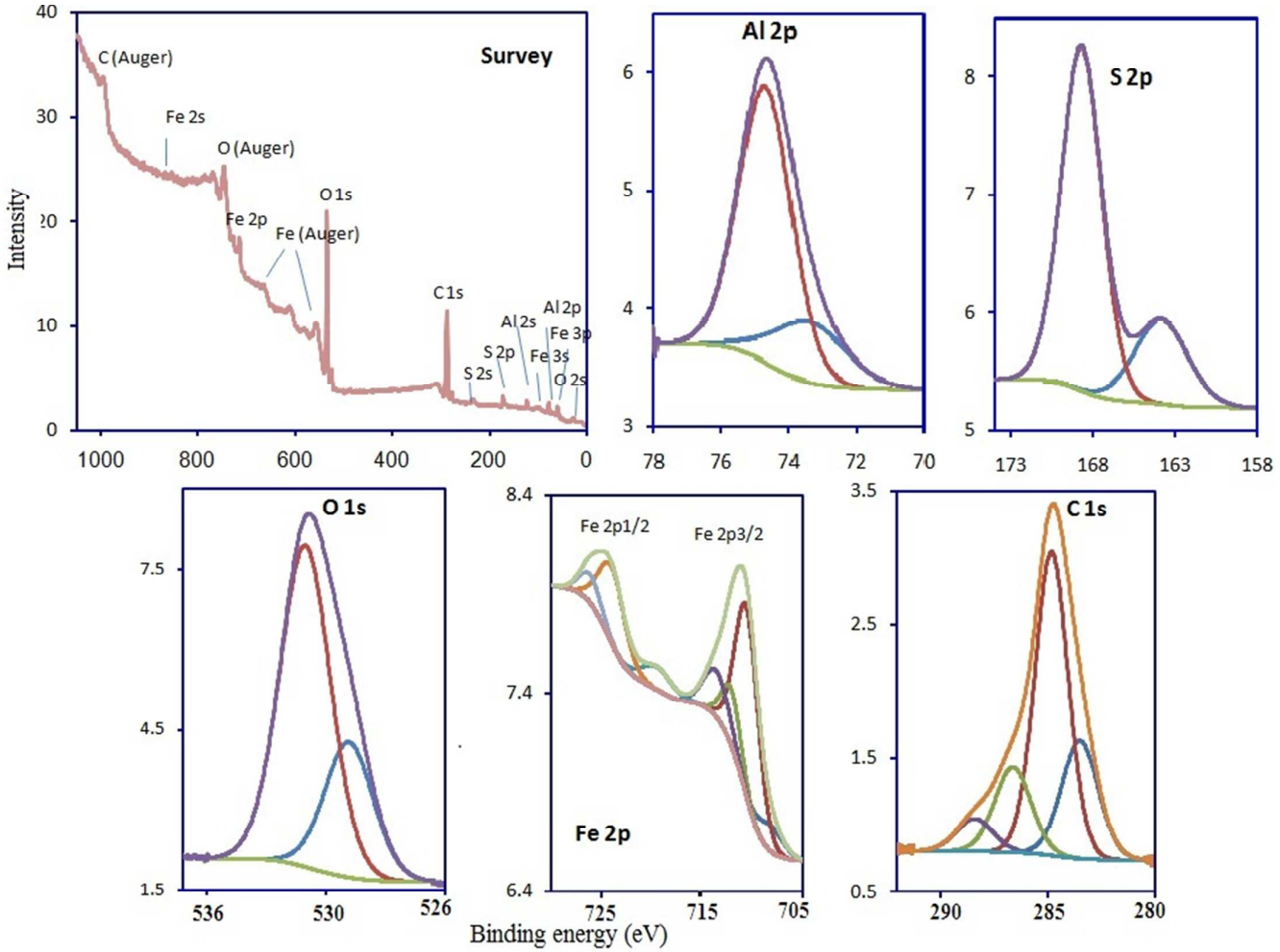

Fig g. 3. XPS analysis of starch/AlOOH/FeS

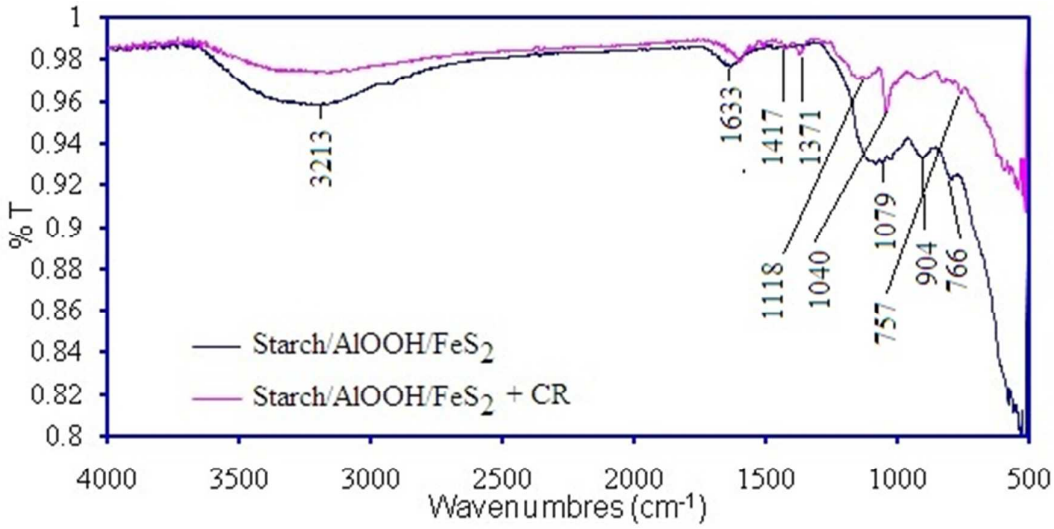

Fig. 4. FTIR spectra of starch/AlOOH/FeS_2 before and after CR adsorption.

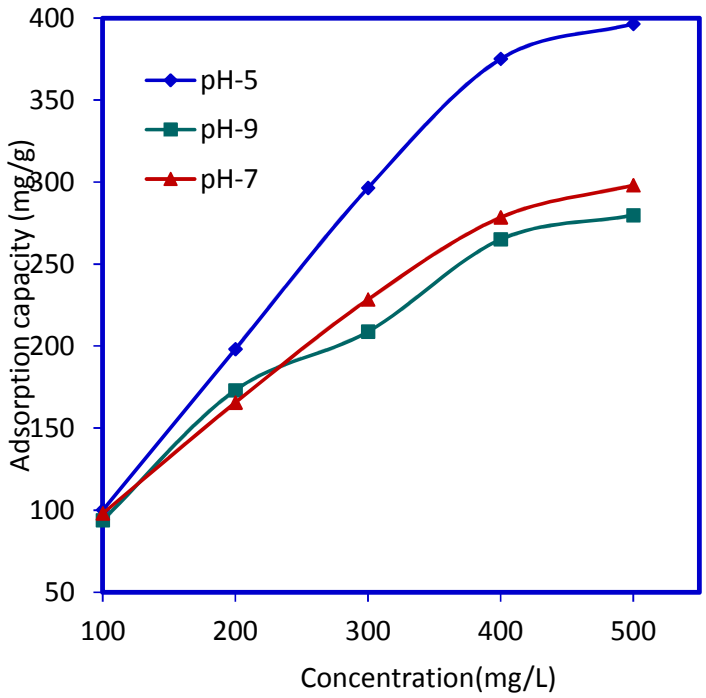

Fig. 5. Effect of solution pH on CR adsorption

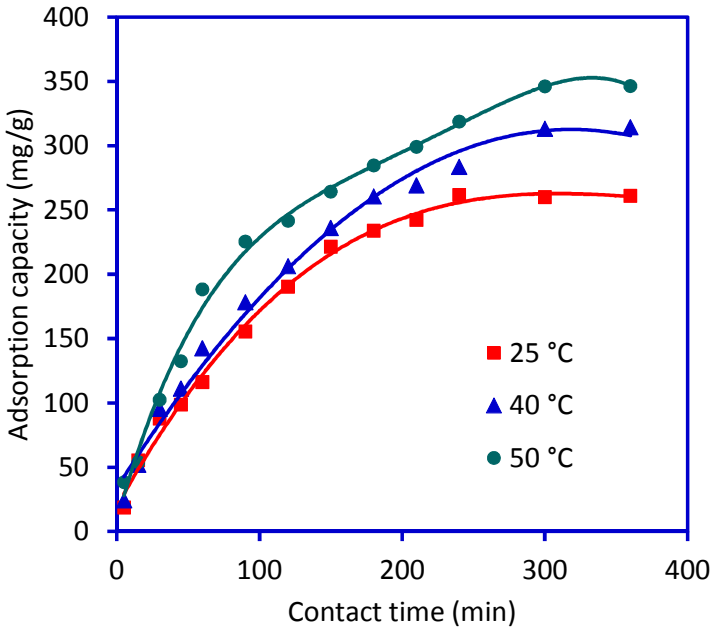

Fig. 6. Effect of Contact time on CR adsorption

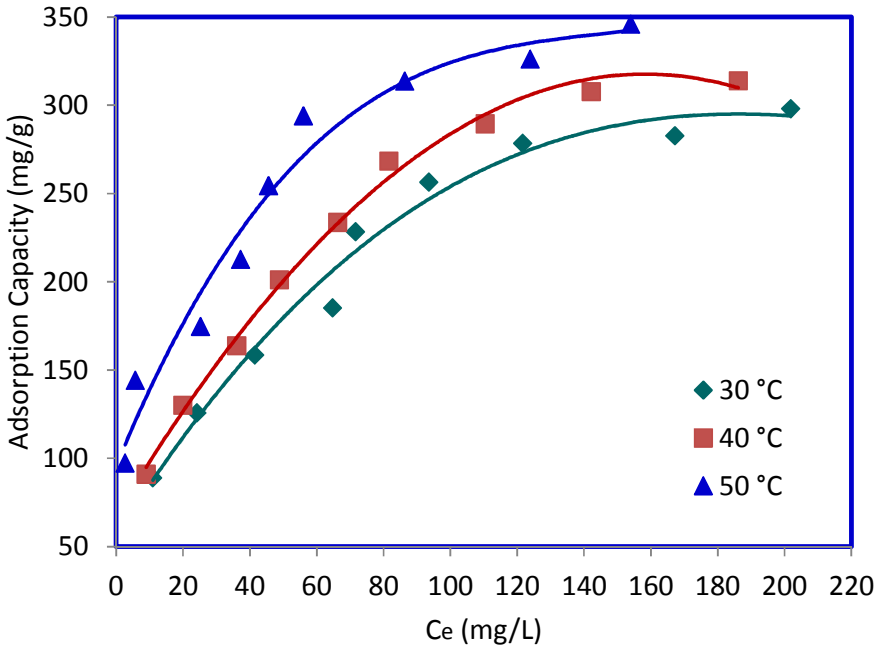

Fig. 7. Effect of concentration of CR adsorption.